Sajed, D. S. et. al. (2017). Diffuse staining for activated NOTCH1 correlates with NOTCH1 mutation status and is associated with worse outcome in adenoid cystic carcinoma. The American Journal of Surgical Pathology, 2017. http://dx.doi.org/10.1097/PAS.0000000000000945.

UNIVERSITY of the WESTERN CAPE

Diffuse staining for activated NOTCH1 correlates with NOTCH1 mutation status and is associated with worse outcome in adenoid cystic carcinoma

Dipti P. Sajed, William C. Faquin, Chris Carey, Eric A. Severson, Amir H. Afrogheh, Carl A. Johnson, Stephen C. Blacklow, Nicole G. Chau, Derrick T. Lin, Jeffrey F. Krane, Vickie Y. Jo, Joaquín J. Garcia, Lynette M. Sholl, and Jon C. Aster

Abstract

NOTCH1 is frequently mutated in adenoid cystic carcinoma (ACC). To test the idea that immunohistochemical (IHC) staining can identify ACCs with NOTCH1 mutations, we performed IHC for activated NOTCH1 (NICD1) in 197 cases diagnosed as ACC from 173 patients. NICD1 staining was positive in 194 cases (98%) in 2 major patterns: subset positivity, which correlated with tubular/cribriform histology; and diffuse positivity, which correlated with a solid histology. To determine the relationship between NICD1 staining and NOTCH1 mutational status, targeted exome sequencing data were obtained on 14 diffusely NICD1-positive ACC specimens from 11 patients and 15 subset NICD1-positive ACC specimens from 15 patients. This revealed NOTCH1 gain-of-function mutations in 11 of 14 diffusely NICD1-positive ACC specimens, whereas all subset positive tumors had wild-type NOTCH1 alleles. Notably, tumors with diffuse NICD1 positivity were associated with significantly worse outcomes ($P = 0.003$). To determine whether NOTCH1 activation is unique among tumors included in the differential diagnosis with ACC, we performed NICD1 IHC on a cohort of diverse salivary gland and head and neck tumors. High fractions of each of these tumor types were positive for NICD1 in a subset of cells, particularly in basaloid squamous cell carcinomas; however, sequencing of basaloid squamous cell carcinomas failed to identify NOTCH1 mutations. These findings indicate that diffuse NICD1 positivity in ACC correlates with solid growth pattern, the presence of NOTCH1 gain of function mutations, and unfavorable outcome, and suggest that staining for NICD1 can be helpful in distinguishing ACC with solid growth patterns from other salivary gland and head and neck tumors.

Adenoid cancer other secrecystic carcinoma (ACC) is an uncommon that usually arises in the salivary glands or tory glands of the head and neck, upper airways, and breast (for recent review, see Dillon et al[1]). Although most cases are slow growing, ACC has a propensity for local spread due to perineural invasion and often ultimately metastasizes, most commonly to the lung, bone, and liver. Local or distal recurrence

after surgical resection, with or without radiation therapy, is common, and for these patients the prognosis is poor, even with aggressive chemotherapy regimens.

ACC has several growth patterns, including tubular, cribriform, and solid. Tumors with tubular/cribriform growth patterns are composed of mixtures of p63-positive myoepithelial cells and KIT-positive epithelial cells, which form luminal or gland-like structures. By contrast, tumors with solid growth patterns are comprised mainly of KIT-positive epithelial cells and have been associated with worse outcomes.[2–5] Many ACCs show a mixture of growth patterns, and some studies suggest that even a minor tumor component showing a solid growth pattern imparts a less favorable prognosis.[5]

Notch receptors participate in a conserved signaling pathway that regulates many cell fate decisions and has diverse cell lineage dependent effects on cellular behavior (for recent review, see Bray[6]). Notch signaling depends of successive ligand-induced cleavages. The first is carried out by ADAM metalloproteases, which cleave at a site within the juxtamembrane negative regulatory region of Notch. This sets the stage for a second cleavage carried out by gamma-secretase, which allows the intracellular portion of Notch to translocate to the nucleus and turn on Notch target genes. Genes encoding Notch receptors and other components of the Notch pathway are recurrently mutated in many cancers, including ACC.[7–11] We recently noted in a small series of primary ACCs and patient derived xenograft models that epithelial differentiation in ACC is associated with activation of NOTCH1,[12–14] as assessed by immunohistochemical (IHC) staining with a rabbit monoclonal antibody specific for a neoepitope located at the N-terminus of the NOTCH1 intracellular domain (NICD1) that is created when NOTCH1 is activated by gamma-secretase cleavage.[15] These findings suggested that IHC staining for NICD1 might provide a simple, rapid, and inexpensive means of identifying NOTCH1-mutated ACCs with solid growth patterns, a subtype that can be diagnostically challenging, particularly in small biopsies with limited tumor sampling. In this study, we tested these ideas by performing NICD1 IHC on a large cohort of ACC specimens as well as a panel of epithelial salivary gland and head and neck tumors. We find that NICD1 staining is a common feature among the diverse tumors studied, but that diffuse NICD1 positivity, which correlates with the presence of NOTCH1 gain-of-function mutations, is restricted to ACCs with solid growth patterns. Notably, we also find that ACCs with diffuse NICD1 positivity in our cohort are associated with a worse outcome. These studies suggest that IHC for NICD1 is useful in identifying ACCs with pathogenic mutations in NOTCH1 and has value as a prognostic marker.

Materials and methods

Cases

Formalin-fixed paraffin-embedded (FFPE) samples were obtained from the tissue archives of Massachusetts General Hospital and Brigham and Women's Hospital with

Institutional Review Board approval. FFPE samples were cut at 4 μm thickness, transferred to Superfrost Plus charged slides, and baked for 60 minutes at 60°C before IHC. Tumors were characterized for growth pattern as tubular/cribriform, solid, mixed tubular/cribriform, and solid, or too scant to reliably assess growth pattern. Case characteristics are summarized in Table 1.

TABLE 1. Characteristics of ACC Cases Selected for Study

No. Patients	Sex	Age (y)	No. Specimens	Tumor Origin	Specimens Subjected to IHC Staining	Growth Pattern
173	Female (111) Male (62)	Range: 12-89 Median: 56	197	Head and neck (major and minor salivary gland) (108); upper airway (60); breast (2); prostate (2); thyroid (1)	Head and neck (primary or local recurrence, 99); upper airway (primary or local recurrence, 54); thyroid (primary, 1); breast (primary, 2); metastatic lesions (41)	Tubular/cribriform (145); solid (16); mixed (16); scant, cannot assess (20)

TABLE 2. Relationship Between Growth Pattern and NICD1 Staining Pattern in ACC

Growth Pattern	NICD1 Staining Pattern
Tubular/cribriform (145)	Subset positive (141, 97.2%) Diffusely positive (1) Subset and focally diffusely positive (1) Negative (2)
Solid (16)	Diffusely positive (13, 81.3%) Subset positive (2) Negative (1)
Tubular/cribriform and solid (16)	Subset positive (6) Subset and focally diffusely positive (4) Diffusely positive (6)

Immunohistochemistry

To explore the association between NOTCH1 activation and histologic features in ACC, we performed immunohistochemistry on 197 FFPE cases diagnosed as ACC from 173 patients.[15] IHC was carried out on a Leica Bond III automated immunostainer following Bond Epitope Retrieval 2 for 40 minutes. NICD1 staining was performed using rabbit monoclonal antibody clone D3B8 (Cell Signaling Technologies, Beverly, MA) at 1:50 for 60 minutes. Staining with diaminobenzidine was developed using the Bond Polymer Refine Detection Kit (Leica). Slides were counterstained with hematoxylin. Scoring of IHC results (negative, subset positive, or diffusely positive) was done independently by J.C.A. and by W.C.F. and D.P.S. Diffuse positivity was defined as staining in >90% of cells within a high power (40×) field in an immunoreactive area of the tumor (judged by positive NICD1 staining in endothelial cells, which constitute an internal positive control[15]). Subset positivity was defined as staining in <90% of cells within a high power (40×) field within immunoreactive areas of the tumor, while negative was defined as the absence of staining in tumor cells within immunoreactive areas of the tumor.

Next-generation Targeted Exome Sequencing

Next-generation sequencing was performed on all ACCs with diffuse NICD1 staining for which adequate viable FFPE samples were available (n = 15), as well as 15 ACCs with subset NICD1 staining, which were selected at random based on tissue availability. Targeted exome

sequencing was performed using an NGS assay (OncoPanel) that detects somatic mutations, copy number variations, and structural variants in tumor DNA extracted from FFPE samples.16,17 The assay covers the exonic sequences of 300 cancer genes and also surveys 113 introns across 35 genes for genomic rearrangements. Areas of tumor in unstained slides were manually removed with a razor blade and used for DNA isolation. DNA (200 ng) was enriched for sequences of interest using a solution phase Agilent SureSelect hybrid capture kit and then used for library preparation. Libraries were sequenced on an Illumina HiSeq 2500 sequencer. Sequence reads were aligned to human reference genome GRCh37 (hg19) with the Burrows-Wheeler Alignment tool.[18] Aligned data were sorted, duplicate marked, and indexed with Picard tools. Base-quality score recalibration and local realignment around insertions and deletions was achieved with the Genome Analysis Toolkit.[19,20] Single nucleotidevariants were called with MuTect.[21] Copy number alterations were determined by comparing normalized sample depth of coverage against a median from a panel of normal samples using an internally developed algorithm (RobustCNV). Structural variants were detected from aligned sequence data using BreaKmer [17]

Nanostring Analysis

To detect truncated NOTCH1 mRNA transcripts in ACC biopsies, an antisense probe set was designed and synthesized by Nanostring that included probes specific for individual exons or spliced exon pairs spanning exons 2 to 34 of NOTCH1. RNA was isolated from paraffin sections containing ACC using an RNeasy FFPE kit (Qiagen). RNA quantified on a NanoDrop spectrophotometer was hybridized to probe sets, captured on an nCounter cartridge, and quantified on a Nanostring Digital Analyzer. nSolver software was used to normalize the data, which was then exported to Excel for further analysis.

Fluorescence In Situ Hybridization

Fluorescence in situ hybridization (FISH) was per- formed according to established methods using a laboratory developed, break-apart probe set for detection of MYB rearrangement. Bacterial artificial chromosomes for probe construction were selected using the University of California Santa Cruz Biotechnology Genome Browser and Database (http://genome.ucsc.edu, genome assembly hg38) and obtained from Invitrogen (Carlsbad, CA). DNA was isolated from bacterial cultures using the Plasmid Maxi Kit (Qiagen, Valencia, CA) and fluorescently labeled via nick translation (Abbott Molecular, Des Plaines, IL). Clone specificity was verified by polymerase chain reaction and by FISH to metaphase chromosome spreads prepared from normal male blood specimens.

Survival Analysis

Patient information was obtained from the electronic medical record of Partners Healthcare under a protocol approved by the Institutional Review Board. Patient vitality was determined from the electronic medical record and from publicly available

information (eg, obituaries). Kaplan-Meier curves were generated with GraphPad Prism 7 software. The significance of differences in survival between groups was assessed using the Log-rank (Mantel-Cox) test.

Results

Relationship between Growth Pattern and NOTCH1 Activation in ACC

Virtually all tumors diagnosed as ACC, regardless of growth pattern, stained positively for NICD1 (Table 2); representative images of NICD1 staining are shown in Figure 1. All but 2 tumors with a tubular/cribriform growth pattern were positive for NICD1 in at least a subset of cells, often in a suprabasilar pattern (Fig. 1A), consistent with prior work showing that p63-positive myoepithelial cells are NICD1 negative.[14] By contrast, 13of 16 ACCs with a solid growth pattern were diffusely positive for NICD1 (81%) (Fig. 1B), whereas tumors with mixed tubular/cribriform and solid growth patterns showed a mixture of NICD1 staining patterns (Table 2), with diffuse NICD1 positivity typically correlating with areas with a solid growth pattern. We also noted, in the process of staining ACCs of salivary gland origin, that normal salivary gland epithelium was uniformly negative for NICD1 (Fig. 1A). Three tumors diagnosed as ACC were completely negative for NICD1 staining. One was a tumor with classic tubular/cribriform ACC morphology. A second NICD1-negative tumor arose in the middle turbinate and exhibited an unusual ribbon-like growth pattern (Fig. 1C). The third NICD1-negative tumor was a lung metastasis from a sinonasal mass that showed basaloid features, nuclear pleomorphism, and focal gland-like microcystic structures (Fig. 1D). Positive staining was observed in internal positive control cells (endothelial cells and/or adjacent benign squamous mucosa) in all 3 of these cases, suggesting that each of these tumors is a true negative.

Diffuse NICD1 Staining Correlates With NOTCH1 Mutation Status in ACC

We hypothesized that ACCs with diffuse NICD1 positivity would be enriched for cases with NOTCH1 gain-of-function mutations. To test this idea, targeted exome sequencing was performed successfully on DNA isolated from 29 FFPE specimens: 14 with diffuse NICD1 positivity and either solid (n = 13) or tubular/cribriform (n = 1) growth patterns; and 15 with subset NICD1 positivity and either tubular/cribriform growth patterns (n = 14) or tubular/cribriform and focally solid growth patterns (n = 1) (Table 3). Diffuse NICD1 positive cases selected for study included 3 different biopsies from 1 patient and 2 different biopsies from a second patient. Of the 14 tumors with diffuse NICD1 positivity, we found that 11 harbored sequence variants within NOTCH1 mutational hotspots (exons 25 to 28, exon 34) that are predicted to produce NOTCH1 gain of function. The observed frequency of NOTCH1 mutations in ACCs from different patients that are diffusely positive for NICD1 (8/11 tumors, or 73%) is substantially higher than the frequency of NOTCH1 mutations that has been observed in NGS studies on unselected ACCs.[7–11] By contrast, none of the 15 tumors with subset positivity for NICD1 had NOTCH1 mutations, a frequency significantly lower than that observed in ACCs with diffuse NICD1 positivity ($P < 0.001$, Fisher exact test).

Different NOTCH1 mutations (n = 11) in this ACC cohort include a range of examples of the 2 major types of gain-of-function mutations previously identified in human cancers: mutations in exons 25 to 28 that lead to ligand-independent NOTCH1 activation[22]; and mutations in exon 34 that result in deletion of the C-terminal NOTCH1 PEST domain. Identified mutations in exons 25 to 28 include 2 mutations in the Lin12-Notch repeats and several point substitutions/deletions in the core of the Notch negative regulatory region (Fig. 2A), as well as 2 in-frame insertions stemming from small duplications (Fig. 2B). In addition, 3 different tumor biopsies from another patient showed loss of NOTCH1 exons 1 to 27 in one allele. This pattern of copy number loss is consistent with the presence of a rearranged, truncated NOTCH1 allele expressing short NOTCH1 transcripts containing only exons 28 to 34, a type of activating mutation described previously in triple negative breast cancer.[13,24] To evaluate this possibility, we performed Nanostring analysis of tumor RNA using a probe set spanning the NOTCH1 locus (Fig. 2C). This revealed excess signal for NOTCH1 exons 28 to 34 relative to exons 1 to 27 in all 3 tumor samples with a 5′ NOTCH1 copy number loss ($P < 0.0001$, 2-sided t test) as well as in a control triple negative breast cancer cell line, MB-157, that contains only truncated NOTCH1 alleles.[13] By contrast, samples from ACCs without NOTCH1 genomic copy number variation lacked NOTCH1 RNA 5′/3′ exon imbalances.

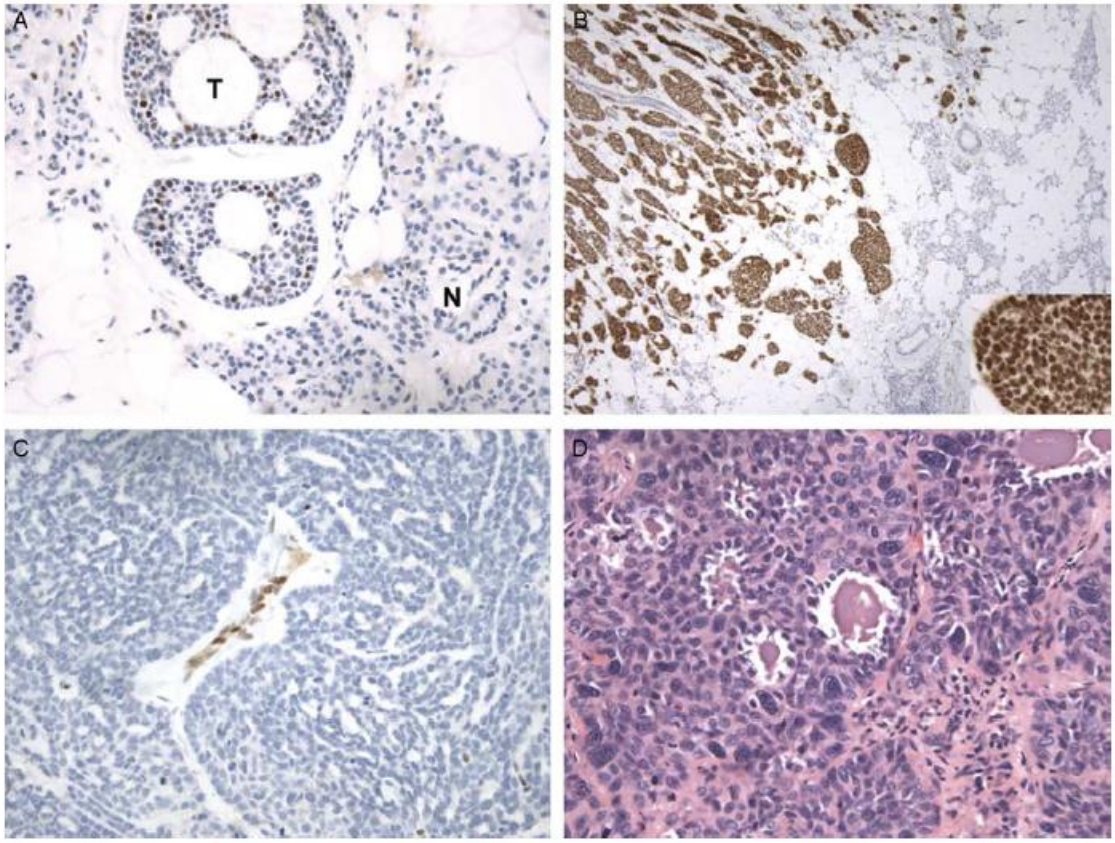

FIGURE 1. Histologic correlates of NICD1 staining in selected cases diagnosed as ACC. A, NICD1 staining in a tubular/cribriform ACC (hematoxylin counterstain). The field contains several nests of tubular/cribriform ACC showing typical subset NICD1 staining (T) adjacent to normal parotid gland (N), which is NICD1 negative. B, Diffuse NICD1 positivity in a solid ACC. Low-power view demonstrates infiltration of normal salivary gland by an ACC with a solid growth pattern and strong, diffuse NICD1 positivity; note nuclear staining in the high-power inset image. C, Absence of NICD1 staining in a tumor diagnosed as ACC involving the middle turbinate showing a ribbon-like or trabecular to solid growth pattern. Other areas in this tumor showed a tubular/cribriform growth pattern reminiscent of ACC. Note NICD1 staining in endothelial cells, which provide an internal control for immunoreactivity. D, H&E-stained section of a NICD1-negative tumor diagnosed as ACC showing squamoid differentiation and microcystic areas.

TABLE 3. Tumor Characteristics and Targeted Exome Sequencing Results in ACC

Tumor Number	NICD1 Staining Pattern	Tumor Location/ Type	Growth Pattern	*NOTCH1* Mutations	Additional Mutations/Aberrations (Affected Gene or Chromosomal Region)
1	Diffuse	Lung (metastasis)	Tubular/ cribriform	None	*PTEN*
2	Diffuse	Thyroid (primary)	Solid	*NOTCH1* c.7507C > T (p.Q2503*), exon 34 in 57% of 38 reads	*PIK3CA*
3	Diffuse	Parotid gland (primary)	Solid	*NOTCH1* c.7400_7400C > GTC (p.S2467fs), exon 34 in 24% of 41 reads	*PIK3CA*
4	Diffuse	Trachea (primary)	Solid	*NOTCH1* c.4744_4747CCGG > G (p. P1582del), exon 26 in 36% of 131 reads	None
5	Diffuse	Trachea (primary)	Solid	*NOTCH1* c.5162T > G (p.V1721G), exon 27 in 38% of 113 reads; *NOTCH1* c.7400C > A (p.S2467*), exon 34 in 45% of 57 reads	None
6	Diffuse	Oropharynx	Solid	None	None
7-9	Diffuse (×3)	Trachea×3 (primary +2 recurrences)	Solid (×3)	One copy loss of *NOTCH1* exons 1-27 (×3)	6q loss except *MYB* exons 1-15
10	Diffuse	Maxillary sinus (primary)	Solid	*NOTCH1* c.4631A > C (p.H1544P), exon 26 in 60% of 81 reads; *NOTCH1* c7398_7399GT > T (p.2466fs), exon 34 in 55% of 58 reads	*ARID1A*, *CREBBP*, 6q abnormality involving *MYB*
11	Diffuse	Liver (metastasis)	Solid	*NOTCH1* c.4680C > A (p.D1560E), exon 26 in 57% of 49 reads	*ARID1A*, *KDM6A*
12	Diffuse	Nasopharynx (primary)	Solid	None	None
13-14	Diffuse (×2)	Trachea (primary) +liver (metastasis)	Solid (×2)	*NOTCH1* exon 27 duplication (primary), *NOTCH1* exon 28 duplication (liver metastasis)	*ARID1A* (trachea); *PMS2* (both biopsies)
15	Subset	Maxillary sinus (recurrence)	Tubular/ cribriform	None	Low copy number gain of 9q34.3
16	Subset (focally diffuse)	Submandibular gland (primary)	Tubular/ cribriform and solid (focal)	None	Single copy number loss of 9q34.3
17	Subset	Maxillary sinus, orbit (recurrence)	Tubular/ cribriform	None	Numerous copy number changes
18	Subset	Submandibular gland (primary)	Tubular/ cribriform	None	None
19	Subset	Pleura (metastasis)	Tubular/ cribriform	None	None
20	Subset	Palate (primary)	Tubular/ cribriform	None	*NFIB-MYB* fusion
21	Subset	Lung (metastasis)	Tubular/ cribriform	None	Numerous copy number variants
22	Subset	Lung (metastasis)	Tubular/ cribriform	None	*MYB-NFIB* fusion; del 22q11.21
23	Subset	Liver (metastasis)	Tubular/ cribriform	None	*CREBP* c.4557C > A (p.Y1519*), exon 27 in 19% of 296 reads; low copy number gain of 9q34.3 and 6q23.3 (*MYB*)
24	Subset	Parotid (primary)	Tubular/ cribriform	None	*TP53*, numerous copy number variants
25	Subset	Trachea (primary)	Tubular/ cribriform	None	*MUTYH*
26	Subset	Lung (metastasis)	Tubular/ cribriform	None	*PIK3CA*, *RUNX1*
27	Subset	Lung (metastasis)	Tubular/ cribriform	None	*ARID2*
28	Subset	Lung (metastasis)	Tubular/ cribriform	None	*NRAS*, *ARID1A*, *KDM6A*
29	Subset	Parotid (primary)	Solid	None	None

Average read coverage, *NOTCH1*: exon 25, 106 (range, 35 to 230); exon 26, 98 (range, 28 to 216); exon 27, 146 (range, 50 to 291); exon 28, 94 (range, 27 to 242); exon 34, 94 (range, 31 to 213).

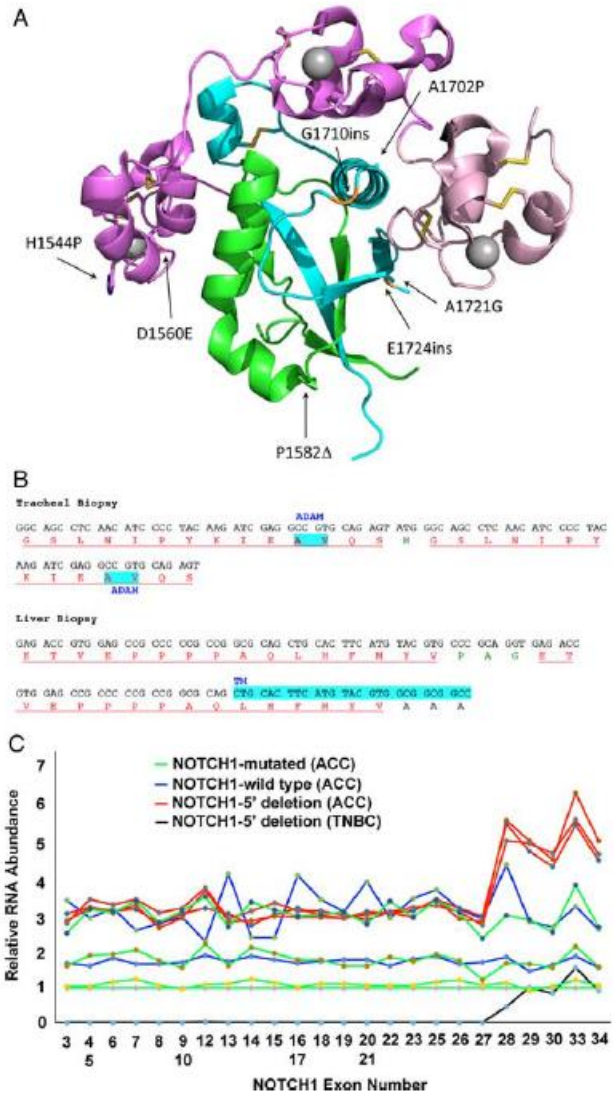

FIGURE 2. *NOTCH1* mutations in ACC. A, Positions of point substitutions and in-frame indels in the NOTCH1 extracellular negative regulatory region. NOTCH1 structure is modeled based on x-ray crystallographic studies of Gordon et al.[23] B, Sequence of juxtamembrane insertional mutations caused by small *NOTCH1* duplications in biopsies of ACC involving the trachea and liver in the same ACC patient. Residues in red correspond to duplicated amino acid residues; residues in green correspond to unique intervening amino acid residues; and residues in black correspond to normal, unduplicated amino acid residues. Highlighted AV residues in the sequence from the tracheal biopsy corresponds to the normal site of ADAM cleavage in NOTCH1, while highlighted residues in the sequence from the liver biopsy corresponds to the NOTCH1 transmembrane domain. C, Nanostring analysis of RNA isolated from FFPE ACC tissue. RNA was isolated from 2 specimens containing ACCs with wild-type *NOTCH1* alleles; 4 ACC specimens with *NOTCH1* alleles with point substitutions or small indels (NOTCH1 mutated); 3 ACC specimens with loss of copy number spanning *NOTCH1* exons 1 to 27; and the triple negative breast cancer cell line MB-157, which has homozygous or hemizygous *NOTCH1* rearrangements and lacks *NOTCH1* exons 1 to 27.[13] RNA abundance expressed as Nanostring signal strength (*y* axis) for each exon covered by probes spanning the *NOTCH1* locus (*x* axis) was first normalized using average signal strength internal control housekeeping genes and then was expressed relative to signal strength for a *NOTCH1*-mutated ACC with no evidence of allelic imbalance, for which signal strength for each exon was arbitrarily set at 1. Note that excess signals for NOTCH1 exons 28 to 34, which encode the NOTCH1 transmembrane domain and intracellular domain, is seen in the control MB-157 triple negative breast cancer cell line (black) and in the 3 samples (red) prepared from specimens with copy number loss involving exons 1 to 27.

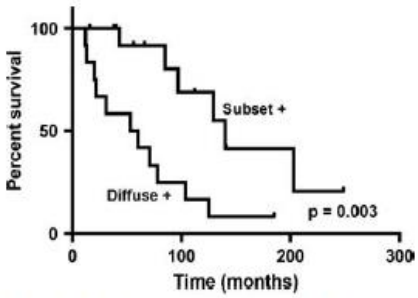

FIGURE 3. Kaplan-Meier survival curves for patients with NICD1 diffusely positive (n=12) or NICD1 subset positive (n=15) ACC.

TABLE 4. Summary of *MYB* Split-apart FISH Results

	MYB FISH Pattern		
NICD1 Staining Pattern	**Normal**	**Rearranged**	**Copy Number Loss**
Diffusely positive (n=9)	0	8	1
Subset positive (n=6)	3	3	0

TABLE 5. NICD1 Staining in Non-ACC Tumors

Diagnosis	No. Cases	Positive NICD1 Staining
Pleomorphic adenoma	22	12/22 (subset)
Epithelioma/ myoepithelioma	9	9/9 (subset)
Basal cell adenoma	22	19/22 (subset)
Basal cell adenocarcinoma	3	2/3 (subset)
Polymorphous low-grade adenocarcinoma	17	7/17 (subset)
bSCC	13	13/13 (often strong staining, major subset of cells)

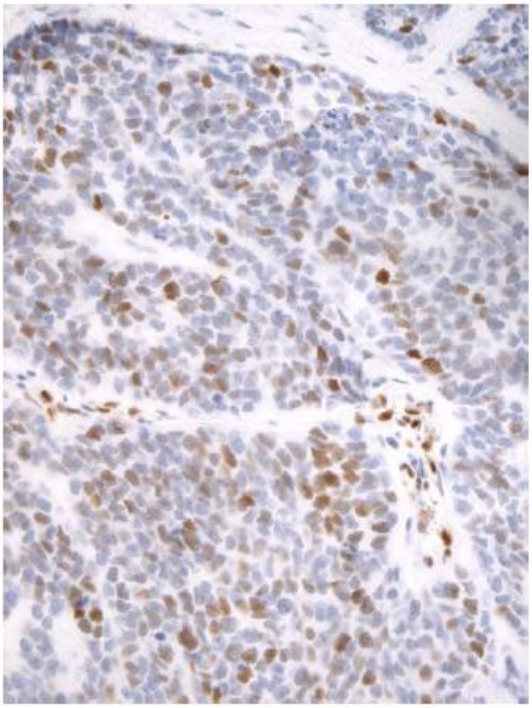

FIGURE 4. Immunohistochemical staining for NICD1 in a representative case of bSCC.

TABLE 6. bSCC NGS Results

Case #	Pathogenic Mutations	CNVs	*MYB* FISH Results
1	*FBXW7 c.1513C>A (p.R505S)*—in 23% of 327 reads *KIT c.1540G>T (p.E514*)*—in 19% of 197 reads *TET2 c.4354C>T (p.R1452*)*—in 22% of 283 reads	3p11.1-3p22.1 loss 3q12.3-3q27.3 loss 11q14.2-11q23.3 loss 13q12.2-13q33.1 loss	Normal
2	*TP53 c.568C>A (p.P190T)*—in 65% of 136 reads *EED c.322_323insGA (p.D109Efs*4)*—in 51% of 446 reads *ARID1B c.956G>T (p.G319V)*—in 62% of 27 reads *FGFR1 c.1615G>A (p.G539R)*—in 48% of 286 reads *IKZF3 c.244G>A (p.E82K)*—in 51% of 346 reads *KDM6B c.485C>T (p.S162F)*—in 15% of 106 reads	Complex gains and losses involving chromosomes 1, 2, 3, 4, 6, 8, 9, 10, 11, 12, 13, 14, 16, and 17	Polysomy
3	*TP53 c.404G>A (p.C135Y)*—in 91% of 275 reads *GNAQ c.524C>T (p.T175M)*—in 47% of 270 reads *KDM5C c.1879C>T (p.R627C)*—in 94% of 100 reads *PIK3CA c.652G>C (p.E218Q)*—in 30% of 725 reads *STAG1 c.3595G>A (p.E1199K)*—in 19% of 575 reads	Complex gains and losses involving chromosomes 2, 3, 5, 7, 8, 9, 11, 13, 14, 15, 16, 17, 18, 20, and X	Polysomy
4	*TP53 c.482C>A (p.A161D)*—in 67% of 369 reads	Complex gains and losses involving chromosomes 2, 3, 4, 5, 7, 8, 9, 11, 12, 14, 15, 17, 19, 20, and X	Polysomy
5	None	Complex gains and losses involving chromosomes 1, 2, 3, 4, 5, 9, 10, 11, 12, 13, and 18	Normal
6	*TP53 c.503_525delACATGACGGAGGTTGTGA GGCGC (p.H168Lfs*5)*—in 22% of 413 reads *CDKN2A c.172C>T (p.R58*)*—in 33% of 105 reads *CDKN2A c.238C>T (p.R80*)*—in 25% of 185 reads *SMARCA4 c.3403C>G (p.R1135G)*—in 26% of 230 reads *CYLD c.1609_1610delAA (p.K537Efs*5)*—in 30% of 383 reads	Complex gains and losses involving chromosomes 1, 3, 4, 5, 6, 8, 9, 11, 14, 16, 19, and 20	Polysomy
7	None	Complex gains and losses involving chromosomes 4, 6, 9, 10, 11, 12, 14, 16, 18, and 20	Normal
8	*TP53 c.216delC (p.V73Wfs*50)*—in 64% of 139 reads *NOTCH2 c.4822A>T (p.R1608*)*—in 39% of 307 reads	Complex gains and losses involving chromosomes 1, 2, 3, 4, 6, 7, 8, 9, 11, 12, 13, 14, 15, 16, 17, 18, 19, and 20	Polysomy
9	*FBXW7 c.1394G>A (p.R465H)*—in 33% of 254 reads *FGFR3 c.746C>G (p.S249C)*—in 34% of 246 reads *KMT2D c.166C>T (p.Q56*)*—in 31% of 360 reads	3q12.3-3q27.3 gain 4q31.3 gain 6p21 loss 6q15-6q26 loss 13q13.1-33.1 loss 20q11.21-13.32 gain	Monosomy
10	*TP53 c.783-20_795del TCTTTTCCTATCCTGAGTAGTGGTAATC-TACTG*—in 11% of 102 reads *NOTCH1 c.7244_7246delCAC (p.P2415del)*—in 6% of 131 reads *PIK3CA c.1633G>A (p.E545K)*—in 17% of 680 reads *SMAD4 c.1333C>T (p.R445*)*—in 57% of 157 reads	Complex gains and losses involving chromosomes 1, 2, 3, 4, 5, 6, 7, 8, 9, 10, 11, 12, 13, 14, 15, 16, 17, 18, 19, 21, and X	Normal
11	*NOTCH1 c.6321delC (p.H2107Qfs*4)*—in 19% of 338 reads	Complex gains and losses involving chromosomes 1, 2, 3, 5, 6, 9, 12, 13, 16, 17, 19, 20, 22, and X	Polysomy
12	*TP53 c.1010G>T (p.R337L)*—in 85% of 204 reads *ARID1A c.465_471delCCGGAGC (p.S157Lfs*73)*—in 36% of 226 reads *KMT2D c.8401C>T (p.R2801*)*—in 41% of 360 reads	Complex gains and losses involving chromosomes 1, 2, 3, 5, 6, 7, 8, 9, 10, 11, 12, 13, 14, 15, 17, 18, 19, 20, and X	Polysomy
13	*TCF7L1 c.1071G>A (p.M357I)*—in 25% of 329 reads	Low copy number gains and losses involving chromosomes 1, 3, 4, 16, 20, 22, and X	Rearranged (66% of nuclei)

Average read coverage, *NOTCH1*: exon 25, 230 (range, 133 to 422); exon 26, 196 (range, 123 to 361); exon 27, 282 (range, 181 to 505); exon 28, 222 (range, 120 to 376); exon 34, 182 (range, 113 to 311).

Diffusely NICD1 Positive ACC is Associated with MYB Rearrangements

ACC is often associated with rearrangements involving the MYB gene on chromosome 6p that lead to MYB overexpression.[7,14] To confirm that the subset of ACCs with diffuse NICD1 positivity is associated with MYB gene rearrangements, we performed FISH with "split apart" probes flanking MYB on 9 diffusely NICD1 positive cases, using subset NICD1 positive ACC cases as controls (n = 6). All 9 diffusely NICD1 positive cases produced abnormal hybridization signals (Table 4). In 8 of these cases, the signals were consistent with the presence of a MYB rearrangement, while in 1 case 1 of 2 MYB signals were lost. However, NGS on this case revealed that all of MYB's 15 exons were retained on both alleles (Table 3), indicating that this tumor also contains a MYB

rearrangement rather than a MYB deletion. Thus, MYB gene rearrangements seem to be common in ACCs with diffuse NICD1 positivity.

Diffuse NICD1 Staining Correlates with Outcome in ACC

To determine whether NICD1 staining pattern correlates with outcome, we obtained vitality data for all patients whose tumors were subjected to IHC and NOTCH1 mutational analysis, including one patient on whose tumor attempted sequencing failed. Kaplan-Meier analysis revealed that ACCs with diffuse NICD1 positivity were associated with significantly worse outcome than NICD1 subset positive tumors (median survival of 56.5 vs. 140 mo, P = 0.003) (Fig. 3).

NICD1 Staining and Notch Mutations in Non-ACCs

The differential diagnosis of ACC includes other benign and malignant basaloid epithelial tumors of salivary gland and other regions of the head and neck. Few of these tumors have been subjected to NGS to date, and we, therefore, used NICD1 IHC to screen a diverse group of non-ACCs for tumors that might harbor NOTCH1 gain-of-function mutations. As shown in Table 5, a high fraction of non-ACCs also showed subset NICD1 positivity. Clear-cut diffuse NICD1 positivity was not observed, but we noted that basaloid squamous cell carcinoma (bSCC) often was strongly NICD1-positive in a subset of cells (Fig. 4).

To exclude the occurrence of NOTCH1 gain-of- function mutations in bSCC, a tumor that has not been previously characterized by genomic sequencing, NGS was performed on all 13 cases (Table 6). This revealed that bSCC is commonly associated with TP53 mutations (8/13cases) and with genomic instability marked by segmental gains and losses in numerous chromosomes (all cases), features that are less frequently seen in ACC (Table 3). As a further point of comparison with ACC, FISH analysis also was performed, which identified frequent changes in copy number involving MYB but only identified 1 tumor with a MYB gene rearrangement (Table 3). Three mutations involving Notch genes were identified. One mutation, P2415del, is an in-frame deletion of a proline residue within an unstructured C-terminal NOTCH1 region of unknown functional significance. The other 2 mutations, R1608* and H2107Gfs*4, disrupt regions of NOTCH1 that are required for function and therefore correspond to loss-of-function mutations. Thus, despite frequent evidence of NOTCH1 activation in bSCC, mutational data point to selective pressure for loss of Notch function in this tumor.

Discussion

This study shows that diffuse NICD1 staining is common in ACCs with solid growth patterns, is highly associated with NOTCH1 gain-of-function mutations, and is associated with worse outcomes. Among tumors of salivary gland and head and neck origin, activation of NOTCH1 is a common feature, but only ACCs show diffuse NICD1 positivity and NOTCH1 mutations in a subset of cases, suggesting that the selective pressure for Notch gain-of-function mutations is specific for ACC among this group of

tumors. Prior NGS studies of ACC have identified NOTCH1 gain-of-function mutations in a subset of cases, varying from 0% to 19% (overall 12/172 cases, or 7%).[7–10] By contrast, we detected NOTCH1 mutations in 8 of 11 ACCs (73%) with diffuse NICD1 positivity, suggesting that NICD1 staining is effective at identifying ACCs with dysregulated NOTCH1 signaling.

Our findings add to the weight of evidence implicating Notch signaling in the pathogenesis of ACC and have several translational implications. Among other epithelial cancers, only triple negative breast cancer has been reported to be associated with NOTCH1 gain-of-function mutations.[13,24] The association of ACCs with a solid growth pattern and diffuse NICD1 positivity suggests that NICD1 staining may be of diagnostic utility in this subset of ACCs, particularly in small biopsies, albeit with an important caveat. In reviewing our ACC cohort, we noted that NICD1 staining intensity often varied from area to area and that patchy negative areas were not uncommon. The NICD1 epitope is in an unstructured region of the intracellular domain of NOTCH1,[25] which may make it susceptible to degradation posttumor resection. This limitation is partially mitigated by the existence of internal positive control cells, such as vascular endothelial cells, in virtually all tissue biopsies. Conversely, lack of NICD1 staining in several of our cases may stem from misdiagnosis. One NICD1-negative neoplasm arising in the middle turbinate had an unusual ribbon-like growth pattern, while a second NICD1-negative tumor, a lung metastasis from a sinonasal mass, had a morphology that was reminiscent of HPV-related carcinoma with adenoid cystic-like features.[26] Further work is needed to determine the value of NICD1 staining in the differential diagnosis of epithelial neoplasms. The association of diffuse NICD1 staining and worse outcome also suggests that NICD1 staining is a useful prognostic marker for ACC, an idea that is reinforced by a recent report showing that NOTCH1 mutations are associated with worse outcome in ACC patients.[27] Finally, clinical trials of several Notch pathway inhibitors are underway in patients with relapsed/ refractory ACC. Prior work has shown that high levels of NICD1 in T-cell acute lymphoblastic leukemia (T-ALL) and triple negative breast cancer cell lines correlate with sensitivity to gamma-secretase inhibitors,[13,28] and T-ALLs that have shown the greatest response to gamma-secretase inhibitors in the context of clinical trials have been NOTCH1 mutated.[29,30] Thus, it is possible that diffuse NICD1 positivity may be predictive of tumor response to Notch pathway inhibitors. We acknowledge, however, that while solid growth pattern, NOTCH1 mutation, and diffuse NICD1 staining are associated, these correlations are not uniform in all cases; thus, further work will be necessary to determine which of these markers, alone or in combination, is most informative.

Several of the NOTCH1 mutations we identified in ACC are unusual. Two in-frame insertions due to sequence duplications occurred in a primary tracheal tumor and a liver metastasis from the same patient, suggesting that the genetic background in this tumor predisposed to this rare type of NOTCH1 mutation. A pathogenic mutation also was identified in the mismatch repair gene PMS2 in both specimens, but typical indel

mutations indicative of a mismatch repair defect were not seen in the NGS data sets and the basis for recurrent insertional NOTCH1 mutations in this tumor is unclear. We also noted that 3 of 4 PEST domain mutations fell in codon 2466 or 2467, a site that is mutated at low frequency in other tumors, such as T-ALL.[28] Of note, of 9 NOTCH1 exon 34 mutations re- ported in ACC by other groups, 5 affected codon 2467,[9,10] suggesting that this is a mutational hotspot in ACC. Enrichment for specific PEST domain mutations is not a prominent feature in T-ALL, but is characteristic of chronic lymphocytic leukemia, in which ~90% of mutations are a del(CT) involving codon 2514.[31,32] The same del (CT) mutation also appears to be a mutational hotspot in mantle cell lymphoma.[33] Whether these tumor-specific mutational patterns reflect selective pressure for loss of different C-terminal regions of NOTCH1 in different cell contexts or are a manifestation of differing mutational mechanisms in various tumors remains to be determined.

Our mutational data also sound a note of clinical caution. Three of the identified NOTCH1 gain-of-function mutations, a deletion spanning exons 1 to 27 of NOTCH1 and 2 insertional mutations that reduplicate juxtamembrane sequences, create mutated alleles encoding receptors that are resistant to NOTCH1 inhibitory antibodies[34] that have been tested in clinical trials, including in patients with ACC (NCT02662608); thus, our findings suggest that if inhibitory antibody therapy is to be given, NOTCH1 mutational testing should be carried out to ensure that the tumor is expressing a "targetable" form of NOTCH1. By contrast, because the antibody used to stain NICD1 recognizes a neoepitope created by gamma-secretase cleavage, mutated NOTCH1 receptors in tumors with diffuse NICD1 positivity should be "targetable" by gamma-secretase inhibitors, regardless of the mechanism of NOTCH1 activation.

References

1. Dillon PM, Chakraborty S, Moskaluk CA, et al. Adenoid cystic carcinoma: a review of recent advances, molecular targets, and clinical trials. Head Neck. 2016;38:620–627.
2. Nascimento AG, Amaral AL, Prado LA, et al. Adenoid cysticcarcinoma of salivary glands. A study of 61 cases with clinicopathologic correlation. Cancer. 1986;57:312–319.
3. da Cruz Perez DE, de Abreu Alves F, Nobuko Nishimoto I, et al. Prognostic factors in head and neck adenoid cystic carcinoma. Oral Oncol. 2006;42:139–146.
4. Bjorndal K, Krogdahl A, Therkildsen MH, et al. Salivary adenoid cystic carcinoma in Denmark 1990-2005: outcome and independent prognostic factors including the benefit of radiotherapy. Results of the Danish Head and Neck Cancer Group (DAHANCA). Oral Oncol. 2015;51:1138–1142.
5. van Weert S, van der Waal I, Witte BI, et al. Histopathological grading of adenoid cystic carcinoma of the head and neck: analysis of currently used grading systems and proposal for a simplified grading scheme. Oral Oncol. 2015;51:71–76.
6. Bray SJ. Notch signalling in context. Nat Rev Mol Cell Biol. 2016; 17:722–735.
7. Ho AS, Kannan K, Roy DM, et al. The mutational landscape of adenoid cystic carcinoma. Nat Genet. 2013;45:791–798.
8. Stephens PJ, Davies HR, Mitani Y, et al. Whole exome sequencing of adenoid cystic carcinoma. J Clin Invest. 2013;123:2965–2968.
9. Ross JS, Wang K, Rand JV, et al. Comprehensive genomic profiling of relapsed and metastatic adenoid cystic carcinomas by next- generation sequencing reveals potential new routes to targeted therapies. Am J Surg Pathol. 2014;38:235–238.
10. Morris LG, Chandramohan R, West L, et al. The molecular landscape of recurrent and metastatic head and neck cancers: insights from a precision oncology sequencing platform. JAMA Oncol. 2016. doi: 10.1001/jamaoncol.2016.1790. [Epub ahead of print].
11. Rettig EM, Talbot CC Jr, Sausen M, et al. Whole-genome sequencing of salivary gland adenoid cystic carcinoma. Cancer Prev Res (Phila). 2016;9:265–274.
12. Persson M, Andren Y, Mark J, et al. Recurrent fusion of MYB and NFIB transcription factor genes in carcinomas of the breast and head and neck. Proc Natl Acad Sci U S A. 2009;106:18740–18744.
13. Stoeck A, Lejnine S, Truong A, et al. Discovery of biomarkers predictive of GSI response in triple-negative breast cancer and adenoid cystic carcinoma. Cancer Discov. 2014;4:1154–1167.
14. Drier Y, Cotton MJ, Williamson KE, et al. An oncogenic MYB feedback loop drives alternate cell fates in adenoid cystic carcinoma. Nat Genet. 2016;48:265–272.
15. Kluk MJ, Ashworth T, Wang H, et al. Gauging NOTCH1 activation in cancer using immunohistochemistry. PLoS One. 2013;8:e67306.
16. Wagle N, Berger MF, Davis MJ, et al. High-throughput detection of actionable genomic alterations in clinical tumor samples by targeted, massively parallel sequencing. Cancer Discov. 2012;2:82–93.
17. Abo RP, Ducar M, Garcia EP, et al. BreaKmer: detection of structural variation in targeted massively parallel sequencing data using kmers. Nucleic Acids Res. 2015;43:e19.

18. Li H, Durbin R. Fast and accurate short read alignment with Burrows-Wheeler transform. Bioinformatics. 2009;25:1754–1760.
19. DePristo MA, Banks E, Poplin R, et al. A framework for variation discovery and genotyping using next-generation DNA sequencing data. Nat Genet. 2011;43:491–498.
20. McKenna A, Hanna M, Banks E, et al. The Genome Analysis Toolkit: a MapReduce framework for analyzing next-generation DNA sequencing data. Genome Res. 2010;20:1297–1303.
21. Cibulskis K, Lawrence MS, Carter SL, et al. Sensitive detection of somatic point mutations in impure and heterogeneous cancer samples. Nat Biotechnol. 2013;31:213–219.
22. Malecki MJ, Sanchez-Irizarry C, Mitchell JL, et al. Leukemia-associated mutations within the NOTCH1 heterodimerization domain fall into at least two distinct mechanistic classes. Mol Cell Biol. 2006;26:4642–4651.
23. Gordon WR, Roy M, Vardar-Ulu D, et al. Structure of the Notch1-negative regulatory region: implications for normal activation and pathogenic signaling in T-ALL. Blood. 2009;113:4381–4390.
24. Robinson DR, Kalyana-Sundaram S, Wu YM, et al. Functionally recurrent rearrangements of the MAST kinase and Notch gene families in breast cancer. Nat Med. 2011;17:1646–1651.
25. Johnson SE, Ilagan MX, Kopan R, et al. Thermodynamic analysis of the CSL x Notch interaction: distribution of binding energy of the Notch RAM region to the CSL beta-trefoil domain and the mode of competition with the viral transactivator EBNA2. J Biol Chem. 2010; 285:6681–6692.
26. Bishop JA, Ogawa T, Stelow EB, et al. Human papillomavirus- related carcinoma with adenoid cystic-like features: a peculiar variant of head and neck cancer restricted to the sinonasal tract. Am J Surg Pathol. 2013;37:836–844.
27. Ferrarotto R, Mitani Y, Diao L, et al. Activating NOTCH1 mutations define a distinct subgroup of patients with adenoid cystic carcinoma who have poor prognosis, propensity to bone and liver metastasis, and potential responsiveness to Notch1 inhibitors. J Clin Oncol. 2017;35:352–360.
28. Weng AP, Ferrando AA, Lee W, et al. Activating mutations of NOTCH1 in human T cell acute lymphoblastic leukemia. Science. 2004;306:269–271.
29. Papayannidis C, DeAngelo DJ, Stock W, et al. A phase 1 study of the novel gamma-secretase inhibitor PF-03084014 in patients with T-cell acute lymphoblastic leukemia and T-cell lymphoblastic lymphoma. Blood Cancer J. 2015;5:e350.
30. Knoechel B, Bhatt A, Pan L, et al. Complete hematologic response of early T-cell progenitor acute lymphoblastic leukemia to the γ- secretase inhibitor BMS-906024: genetic and epigenetic findings in an outlier case. Cold Spring Harb Mol Case Stud. 2015;1:a000539.
31. Puente XS, Bea S, Valdes-Mas R, et al. Non-coding recurrent mutations in chronic lymphocytic leukaemia. Nature. 2015;526:519–524.
32. Puente XS, Pinyol M, Quesada V, et al. Whole-genome sequencing identifies recurrent mutations in chronic lymphocytic leukaemia. Nature. 2011;475:101–105.

33. Kridel R, Meissner B, Rogic S, et al. Whole transcriptome sequencing reveals recurrent NOTCH1 mutations in mantle cell lymphoma. Blood. 2012;119:1963–1971.
34. Aste-Amezaga M, Zhang N, Lineberger JE, et al. Characterization of notch1 antibodies that inhibit signaling of both normal and mutated notch1 receptors. PLoS One. 2010;5:e9094.